

University of Massachusetts Medical School
eScholarship@UMMS

GSBS Student Publications

Graduate School of Biomedical Sciences

2014-08-19


Genome-wide mutant fitness profiling identifies nutritional requirements for optimal growth of *Yersinia pestis* in deep tissue

Samantha G. Palace
University of Massachusetts Medical School Worcester

Et al.

Let us know how access to this document benefits you.

Follow this and additional works at: https://escholarship.umassmed.edu/gsbs_sp

 Part of the [Bacteriology Commons](#), [Genomics Commons](#), [Immunology and Infectious Disease Commons](#), and the [Pathogenic Microbiology Commons](#)

Repository Citation

Palace SG, Proulx MK, Lu S, Baker RE, Goguen JD. (2014). Genome-wide mutant fitness profiling identifies nutritional requirements for optimal growth of *Yersinia pestis* in deep tissue. GSBS Student Publications. <https://doi.org/10.1128/mBio.01385-14>. Retrieved from https://escholarship.umassmed.edu/gsbs_sp/1920

Creative Commons License



This work is licensed under a [Creative Commons Attribution-Noncommercial-Share Alike 3.0 License](#). This material is brought to you by eScholarship@UMMS. It has been accepted for inclusion in GSBS Student Publications by an authorized administrator of eScholarship@UMMS. For more information, please contact Lisa.Palmer@umassmed.edu.

Genome-Wide Mutant Fitness Profiling Identifies Nutritional Requirements for Optimal Growth of *Yersinia pestis* in Deep Tissue

Samantha G. Palace,^a Megan K. Proulx,^a Shan Lu,^b Richard E. Baker,^a Jon D. Goguen^a

Department of Microbiology and Physiological Systems^a and Laboratory of Nucleic Acid Vaccines, Department of Medicine,^b University of Massachusetts Medical School, Worcester, Massachusetts, USA

ABSTRACT Rapid growth in deep tissue is essential to the high virulence of *Yersinia pestis*, causative agent of plague. To better understand the mechanisms underlying this unusual ability, we used transposon mutagenesis and high-throughput sequencing (Tn-seq) to systematically probe the *Y. pestis* genome for elements contributing to fitness during infection. More than a million independent insertion mutants representing nearly 200,000 unique genotypes were generated in fully virulent *Y. pestis*. Each mutant in the library was assayed for its ability to proliferate *in vitro* on rich medium and in mice following intravenous injection. Virtually all genes previously established to contribute to virulence following intravenous infection showed significant fitness defects, with the exception of genes for yersiniabactin biosynthesis, which were masked by strong intercellular complementation effects. We also identified more than 30 genes with roles in nutrient acquisition and metabolism as experiencing strong selection during infection. Many of these genes had not previously been implicated in *Y. pestis* virulence. We further examined the fitness defects of strains carrying mutations in two such genes—encoding a branched-chain amino acid importer (*brnQ*) and a glucose importer (*ptsG*)—both *in vivo* and in a novel defined synthetic growth medium with nutrient concentrations matching those in serum. Our findings suggest that diverse nutrient limitations in deep tissue play a more important role in controlling bacterial infection than has heretofore been appreciated. Because much is known about *Y. pestis* pathogenesis, this study also serves as a test case that assesses the ability of Tn-seq to detect virulence genes.

IMPORTANCE Our understanding of the functions required by bacteria to grow in deep tissues is limited, in part because most growth studies of pathogenic bacteria are conducted on laboratory media that do not reflect conditions prevailing in infected animal tissues. Improving our knowledge of this aspect of bacterial biology is important as a potential pathway to the development of novel therapeutics. *Yersinia pestis*, the plague bacterium, is highly virulent due to its rapid dissemination and growth in deep tissues, making it a good model for discovering bacterial adaptations that promote rapid growth during infection. Using Tn-seq, a genome-wide fitness profiling technique, we identified several functions required for fitness of *Y. pestis* *in vivo* that were not previously known to be important. Most of these functions are needed to acquire or synthesize nutrients. Interference with these critical nutrient acquisition pathways may be an effective strategy for designing novel antibiotics and vaccines.

Received 23 May 2014 Accepted 16 July 2014 Published 19 August 2014

Citation Palace SG, Proulx MK, Lu S, Baker RE, Goguen JD. 2014. Genome-wide mutant fitness profiling identifies nutritional requirements for optimal growth of *Yersinia pestis* in deep tissue. *mBio* 5(4):e01385-14. doi:10.1128/mBio.01385-14.

Editor Eric Rubin, Harvard School of Public Health

Copyright © 2014 Palace et al. This is an open-access article distributed under the terms of the [Creative Commons Attribution-Noncommercial-ShareAlike 3.0 Unported license](https://creativecommons.org/licenses/by-nc-sa/4.0/), which permits unrestricted noncommercial use, distribution, and reproduction in any medium, provided the original author and source are credited.

Address correspondence to Jon D. Goguen, jon.goguen@umassmed.edu.

Serendipitous quirks of *Yersinia* biology catalyzed much of the research into the molecular basis of *Y. pestis* pathogenesis in the last three decades. For example, the finding that the addition of skim milk to the growth medium enhanced retention of virulence of *Y. pestis* cultured at 37°C (1) ultimately led to the discovery of type III secretion (2). The identification of the yersiniabactin siderophore system required for bacterial iron acquisition during infection (3, 4) was similarly prefaced by the observation that the ability of *Y. pestis* to form pigmented colonies on medium containing hemin was somehow linked to virulence (5, 6). A large fraction of current research on *Yersinia* virulence centers exclusively on the few virulence determinants discovered by these early efforts. To date, these studies have largely eclipsed more systematic attempts to define virulence determinants and other important factors contributing to severity of disease.

The limitations of previous iterations of whole-genome techniques are partly responsible for this focus. Prior genome-level studies of *Y. pestis* relied on acquisition of gene expression data under various *in vitro* and *in vivo* conditions (7–11). These results provide a deeper understanding of physiological adaptations employed by the bacterium in different environments; however, gene expression data have not proved to be a reliable predictor of virulence determinants (12–14). Attempts to circumvent this problem by directly measuring the functional contribution of *Y. pestis* genes to bacterial growth *in vivo* have been more successful but rely on measuring the fitness of a defined panel of mutants rather than implementing a truly unbiased genome-scale technique (15).

Recently, the combination of transposon mutagenesis and high-throughput sequencing has provided a more direct approach to functional genomics. This method has been assigned several

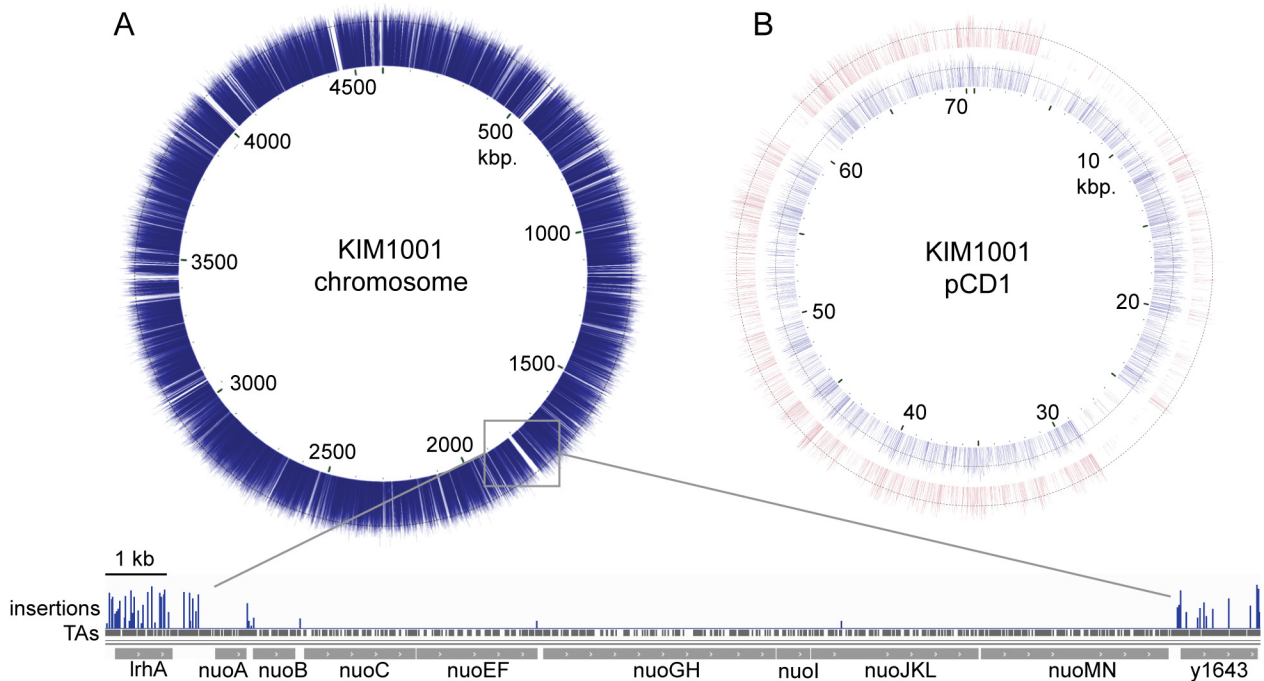


FIG 1 Dense transposon mapping of the *Y. pestis* genome allows identification of regions under selection. The number of insertions sequenced at each site is represented by bar height (log scale). Circular plots were generated using the software program CGView (62). (A) Transposon insertions mapping to the chromosome. Large gaps correspond to blocks of essential genes, such as the NADH dehydrogenase subunits (inset; insertions are shown by the Integrated Genomics Viewer software tool [63, 64] on a log scale). (B) Transposon insertions mapping to the type III secretion plasmid pCD1. Insertions in many genes in the first 30 kb of pCD1, which encode regulatory and structural components of the type III secretion system, are selected against *in vivo* (outer ring; red bars) but not *in vitro* (inner ring; blue bars). The gap of insertions at the 60-kb mark corresponds to plasmid replication genes.

names, including HITS (16), TraDIS (17), INSeq (18), and Tn-seq (19). Tn-seq employs deep sequencing to map and count transposon/genome junctions from a dense library of random transposon insertion mutants grown *en masse* under each condition of interest. The number of transposon insertions detected in a given gene reflects the prevalence of the corresponding mutants in the library following selection (20). This information can be used to estimate relative fitness for mutants in different growth environments.

Tn-seq is an increasingly popular tool in studies of bacterial pathogens (14, 16–31), although to date only five pathogens have been examined using animal infection as a selection regime (*Streptococcus pneumoniae* [23, 26], *Haemophilus influenzae* [16], *Yersinia pseudotuberculosis* [25], uropathogenic *Escherichia coli* [30], and *Mycobacterium tuberculosis* [31]). Here, we used Tn-seq to measure the fitness of nearly 200,000 unique *Y. pestis* insertion mutants during growth *in vitro* in rich culture medium and in mice following intravenous inoculation. We identified several genes contributing to bacterial fitness during infection that had not previously been implicated in virulence, including more than 30 genes with roles in nutrient import and metabolism. The majority of known virulence factors required for optimal bacterial growth during infection were also required in the Tn-seq data set, underscoring the suitability of this method in the context of infection studies.

RESULTS

Transposon mapping of the *Yersinia pestis* genome. We mutagenized the fully virulent *Y. pestis* strain KIM1001 (see Text S1 in

the supplemental material) with a *himar1*-derived transposon to construct a bank of approximately 1.5 million independent insertion mutants. To select against mutants harboring insertions in genes required for growth *in vitro*, the insertion library was grown on TB, a complex medium adapted from tryptose blood agar base that provides a broadly permissive growth condition for insertion mutants.

To select against mutants harboring insertions in genes required for growth during mammalian infection, we performed intravenous infections of three C57BL/6 mice with 2.3×10^7 CFU of the insertion library, which resulted in a population of $\sim 10^6$ bacteria in each spleen 1 h postinfection. This infection route preserves library diversity by circumventing bottlenecks imposed by peripheral routes of infection. Bacteria were recovered from spleens 40 h postinfection by plating on TB agar. Bacterial populations in the spleen at the time of harvest averaged 1.63×10^9 CFU/spleen (ranging from 1.4×10^9 to 2.1×10^9). This population expansion is in excess of 1,000-fold, large enough to permit detection of modest reductions in fitness even in the absence of bacterial killing by host defenses.

Following selection, we mapped the transposon insertions present in the bacterial populations recovered from the *in vitro* and *in vivo* expansions via selective amplification of transposon-genome junctions and Illumina sequencing, using methods similar to those previously described (see Text S1 in the supplemental material). The *himar1* transposon derivative used for mutagenesis inserts at TA dinucleotides (32, 33). Approximately 69% (187,780 of 271,354) of TAs in the *Y. pestis* KIM genome harbored inser-

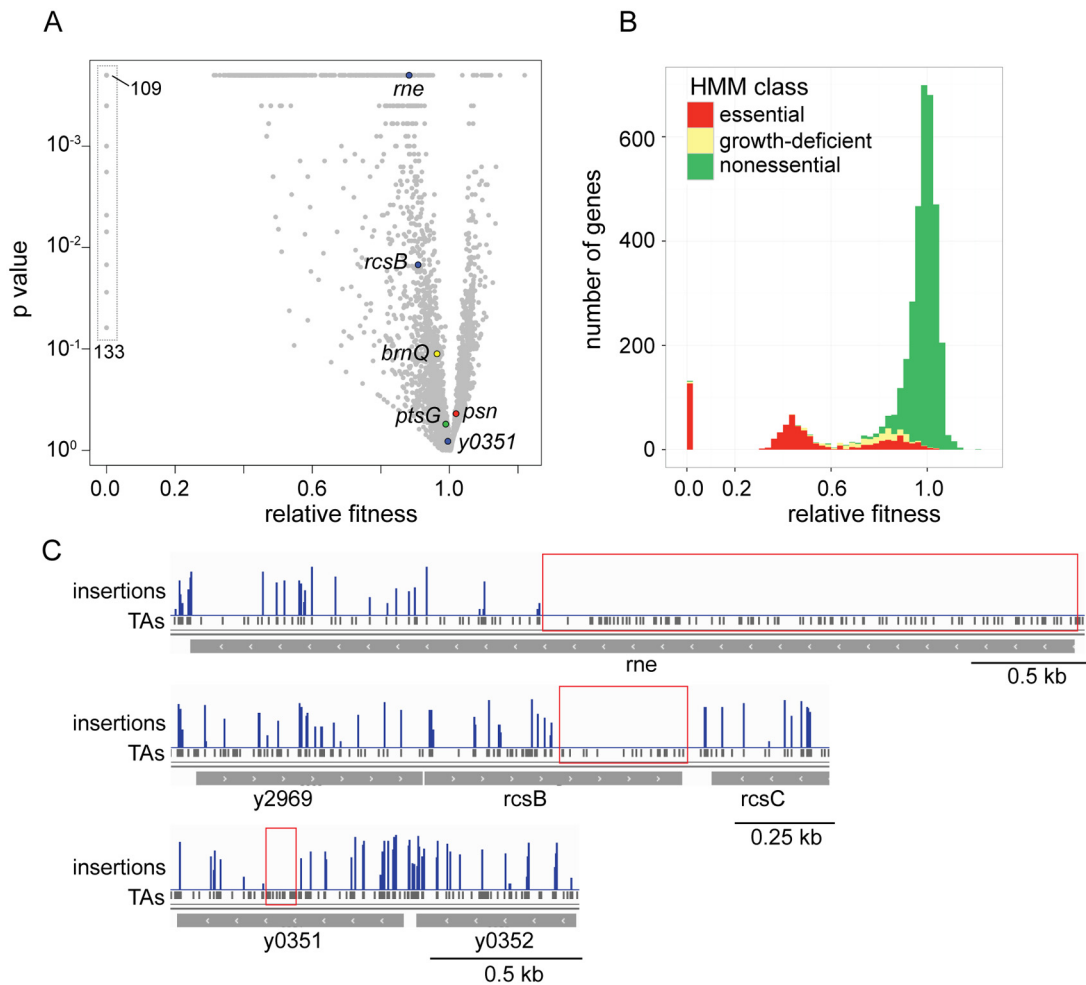


FIG 2 Selection of chromosomal *Y. pestis* genes during growth *in vitro* on rich medium. (A) The relative fitness of mutants in each chromosomal ORF plotted against significance (calculated by resampling; see Text S1 in the supplemental material). Genes harboring no sequenced insertions in the central 90% of the ORF (relative fitness = 0) are shown in the box at the left of the plot. (B) Relative fitness (histogram) correlates well to essentiality, as predicted by the hidden Markov model recently published by DeJesus and Ioerger (36) (red, essential; yellow, growth-deficient; green, nonessential). Genes harboring no sequenced insertions in the central 90% of the ORF (relative fitness = 0) are shown at the left of the plot. (C) Three examples of genes with modest reductions in relative fitness that were predicted to be essential by the hidden Markov model. Many genes in this class contain groups of consecutive TA sites that do not harbor insertions (red boxes), suggesting domain architecture. For example, the apparently essential N terminus of the *rne* gene is highly homologous to the essential *E. coli* gene of the same name (65, 66), while the evidently nonessential C terminus is highly divergent from the *E. coli* homologue, as has been reported for several other species (67); also shown is the apparently essential C-terminal DNA-binding domain of the *rcsB* gene, a transcriptional activator with multiple roles, including small RNA production and cell division (68). Insertions are shown by the Integrated Genomics Viewer software tool (63, 64) on a log scale.

tions, an average density of 39 insertions per kilobase. This high density of insertions allowed fine-scale mapping of functional genetic units, including intergenic regions (Fig. 1A). The density of mutations on pMT1, pCD1, and pPCP1, the three plasmids present in *Yersinia pestis* KIM, was similar to that on the chromosome (78% on pMT1, 76% on pPCP1, and 63% on pPCP1, compared to 69% on the chromosome) (Fig. 1B). Although substantial large-scale heterogeneity in insertion density has been observed after similar transposon mutagenesis of other pathogens (21, 34), insertions in our library were distributed relatively evenly across the chromosome (Fig. 1A).

Identifying genes required for optimal growth *in vitro*. To identify genes required for optimal growth of *Y. pestis* on rich medium, we analyzed the full set of *Y. pestis* KIM open reading frames (ORFs) annotated in the NCBI database by two distinct

mathematical approaches for measuring the effect of insertions on fitness.

In the first approach, we estimated the relative fitness (W) of mutants harboring insertions in each chromosomal ORF, using an analysis similar to that described by van Opijnen and Camilli (35). In the context of evolutionary biology, relative fitness is defined as the ratio of the rates of population expansion for the two genotypes being compared. Mutants with relative fitness of <1 are defective in growth or survival relative to the wild type, while mutants with relative fitness of >1 are more fit than the wild type. To test the statistical significance of the observed changes in fitness for each gene, we employed a nonparametric approach based on a reference distribution created by resampling insertion frequencies in TA sites in nonessential ORFs (defined as those with relative fitness between 0.95 and 1.05) and plotted relative fitness versus

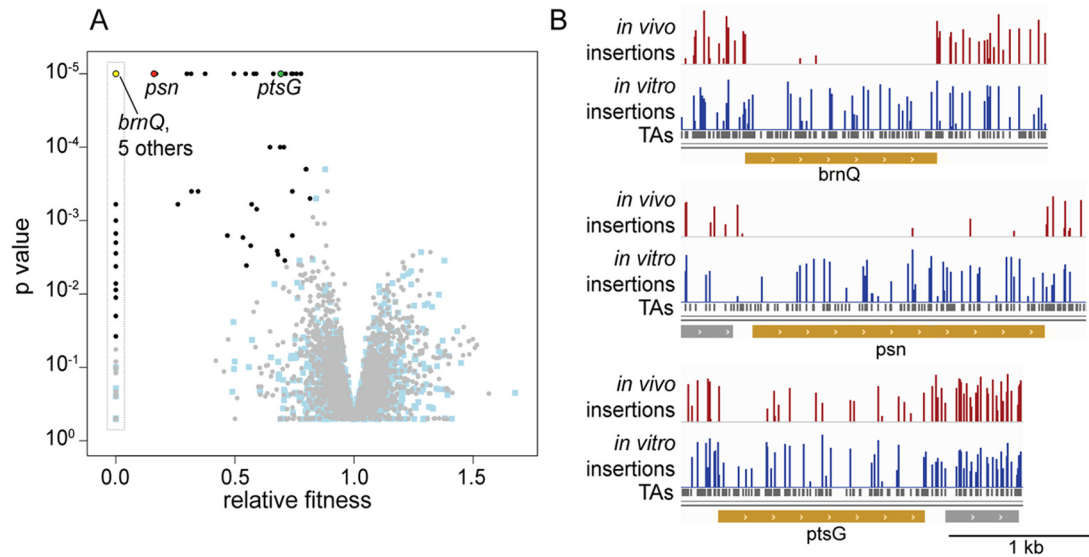


FIG 3 Comparison of Tn-seq data sets to find chromosomal genes required during mammalian infection. (A) Volcano plot for identification of chromosomal genes selected *in vivo*. Each gene was compared between two *in vitro* data sets (filled pale blue squares) or between an *in vitro* data set and the *in vivo* data set (gray circles). Genes experiencing significant selection *in vivo* are represented by black circles. For each gene, relative fitness of insertion mutants *in vivo* is given with respect to the fitness of a wild-type strain. Significance is calculated by permuting the number of insertions sequenced at each TA in the gene between the two data sets (see Text S1 in the supplemental material). Genes selected *in vivo* appear in the upper-left quadrant, while any genes that harbor more insertions *in vivo* than *in vitro* should track to the upper-right quadrant. Genes harboring no sequenced insertions *in vivo* in the central 90% of the ORF (relative fitness = 0) are shown in the box at the left of the plot. (B) Genes experiencing strong selection (*psn* and *brnQ*) harbor many fewer insertions after growth *in vivo*. The same effect is present but less pronounced in genes experiencing moderate levels of selection (*ptsG*). Insertions are shown by the Integrated Genome Viewer tool (63, 64) on a log scale.

significance (Fig. 2A) (for method details, see Text S1 in the supplemental material; for complete results, see Table S1).

A drawback of this first approach is its insensitivity to ORFs containing multiple functional domains with differing contributions to fitness. To address this problem, we used the hidden Markov model (HMM) recently developed by DeJesus and Iorger (36). This method classifies genes as essential, growth disadvantaged, nonessential, or growth advantaged. A complete list of classification of ORFs by the HMM algorithm is available in Table S2 in the supplemental material, and the metabolic pathways most commonly represented by this list of genes, as mapped by the Kyoto Encyclopedia of Genes and Genomes (37), are summarized in Table S3. Relative fitness values were good predictors of HMM class (Fig. 2B), indicating general agreement of these two methods. However, a small number of genes classified as essential or growth deficient by the HMM were assigned relatively high relative fitness values (above 0.75).

In some cases, these results are consistent with known domain structure; this algorithm is particularly sensitive to consecutive TA sites without insertions and therefore correctly classifies ORFs containing subgenic essential domains (Fig. 2C). However, other genes in this group have insertion patterns that render their classification suspect (discussed fully in Text S2 in the supplemental material). These include genes with relatively short (<20) runs of insertion-free TAs, which are less likely to represent functional protein domains, and runs of insertion-free TAs in unusually AT-rich sequences, which may be more difficult to sequence due to base composition bias in library preparation and/or Illumina sequencing (38).

The HMM analysis also identifies some plasmid genes as essential, including genes required for plasmid replication. The

apparent selection on these genes does not stem from any essential function of the plasmids but instead reflects the biological impossibility of propagating insertions that prevent the replication of their host genetic element. The plasmid pCD1, which encodes the *Y. pestis* type III secretion system (T3SS), harbors a second class of genes that the HMM scores as essential or growth deficient. The majority of these are involved in regulating type III secretion (T3S) activity (e.g., *yscM*, *lcrGVH*, and *lcrD*), and insertions in these genes are underrepresented because uncontrolled expression of the T3SS at 37°C *in vitro* inhibits growth of *Y. pestis* (e.g., see reference 39). Curiously, the pattern of T3SS genes selected *in vitro* deviates somewhat from current models of T3S regulation. In particular, the regulatory gene *lcrE* (sometimes called *yopN*) was not subject to significant selection under our *in vitro* condition (falling into the nonessential HMM class), and we observed unexpectedly strong selection against *yopB* mutants *in vitro*. We do not conceive a simple explanation for these unexpected phenotypes and suggest that this regulatory scheme may require further investigation.

Identifying genes selected during infection. Because we were particularly interested in identifying genes required for optimal growth and survival during infection, we calculated the relative fitness of insertion mutants from the *in vivo* Tn-seq data set. To determine whether the period of growth *in vivo* significantly changed the abundance of insertion mutants for each gene, we developed a nonparametric statistic based on a reference distribution created by permuting insertion frequencies in the relevant ORF from both the *in vitro* and *in vivo* data sets (see Text S1 in the supplemental material) and plotted the relative fitness versus significance (Fig. 3A). A complete table of these values is provided in Table S1. Rare genes with substantial reductions in *in vivo* relative

TABLE 1 Chromosomal *Y. pestis* genes experiencing significant selection in deep tissue

Gene name	Gene function	Relative fitness <i>in vivo</i>	<i>P</i> value
<i>arcB</i> (y0126)	Aerobic respiration control	0.798	2.00E-04
y0160	Unknown function	0.681	2.90E-03
<i>pyrB</i> (y0161)	Pyrimidine biosynthesis	0.566	2.20E-03
<i>purD</i> (y0501)	Purine biosynthesis	0.345	4.00E-04
<i>purH</i> (y0502)	Purine biosynthesis	0.316	1.00E-05
<i>miaA</i> (y0629)	IPP transferase to tRNA	0	2.80E-03
<i>hflK</i> (y0633)	FtsH protease regulator	0.738	1.00E-05
y0661	Conserved domain of unknown function	0.647	1.00E-04
<i>pcm</i> (y0832)	Protein L-isoaspartate O-methyltransferase	0.677	2.60E-03
<i>brnQ</i> (y0981)	Branched-chain amino acid import	0	1.00E-05
<i>purK</i> (y1102)	Purine biosynthesis	0.298	1.00E-05
<i>purE</i> (y1103)	Purine biosynthesis	0.261	6.00E-04
<i>purL</i> (y1309)	Purine biosynthesis	0.168	1.00E-05
<i>guaB</i> (y1362)	Purine metabolism	0	6.00E-04
<i>guaA</i> (y1363)	Purine metabolism	0	4.20E-03
<i>purN</i> (y1406)	Purine biosynthesis	0.534	1.70E-03
<i>purM</i> (y1407)	Purine biosynthesis	0	1.50E-03
y1412	Putative zinc-dependent peptidase	0.758	1.00E-05
<i>purC</i> (y1421)	Purine biosynthesis	0	1.00E-03
y1483	Putative histidine kinase sensor	0.661	1.00E-05
<i>purF</i> (y1605)	Purine biosynthesis	0.496	1.00E-05
<i>ptsG</i> (y1767)	Glucose importer	0.693	1.00E-05
<i>ndh</i> (y1777)	NADH dehydrogenase	0.589	1.00E-05
y1920	LPS modification (<i>arnD</i> homologue)	0.317	4.00E-04
y1940	Contains putative L,D-transpeptidase domain	0.548	4.10E-03
<i>tonB</i> (y2037)	Membrane transport	0	1.12E-02
<i>pyrF</i> (y2069)	Pyrimidine biosynthesis	0	2.00E-02
<i>ybtP</i> (y2397)	Siderophore import	0	3.78E-02
<i>ybtA</i> (y2398)	Regulator of siderophore biosynthesis/import	0	1.00E-05
<i>psn</i> (y2404)	Siderophore import	0.160	1.00E-05
<i>cycA</i> (y2447)	D-Alanine/D-serine/glycine permease	0.709	3.50E-03
<i>pabB</i> (y2535)	<i>para</i> -aminobenzoate synthesis	0.690	1.00E-04
<i>aroP</i> (y2564)	Aromatic amino acid import	0.777	1.00E-05
<i>hisF</i> (y2627)	Histidine biosynthesis	0.570	6.00E-04
y2739	Putative ATP-dependent protease	0.591	7.00E-04
<i>aspC</i> (y2760)	Amino acid metabolism/biosynthesis	0.706	1.00E-04
<i>aroA</i> (y2783)	Aromatic amino acid biosynthesis	0	2.00E-03
<i>cydD</i> (y2803)	Cysteine/glutathione transport	0.799	2.00E-04
<i>cydC</i> (y2805)	Cysteine/glutathione transport	0.815	5.00E-04
<i>nrdA</i> (y2974)	Nucleotide biosynthesis	0.713	1.00E-05
<i>nrdB</i> (y2975)	Nucleotide biosynthesis	0	1.00E-05
<i>metN</i> (y3104)	Methionine transport	0	1.00E-05
y3105	Methionine transport	0	1.00E-05
<i>metQ</i> (y3106)	Methionine transport	0	1.00E-05
<i>tbpA</i> (y3651)	Thiamine transport	0.545	1.00E-05
<i>thiP</i> (y3652)	Thiamine transport	0.742	1.00E-05
<i>thiQ</i> (y3653)	Thiamine transport	0	7.20E-03
<i>nhaA</i> (y3704)	Na ⁺ /H ⁺ antiporter	0.375	1.00E-05
y3803	GTP-binding factor	0.741	4.00E-04
<i>hemN</i> (y3807)	Porphyrin metabolism	0.579	1.00E-05
<i>envZ</i> (y3917)	Histidine kinase osmosensor	0.741	1.60E-03
<i>pabA</i> (y3953)	<i>para</i> -aminobenzoate synthesis	0.468	1.60E-03
<i>aroE</i> (y4028)	Aromatic amino acid biosynthesis	0	8.80E-03

fitness that do not reach significance (Fig. 3A, lower left of plot) are associated with large growth defects both *in vitro* and *in vivo* (see Text S1).

The PCR amplification and Illumina sequencing steps required for Tn-seq introduce variability into the measured relative abundance of each mutant in the library, leading to differences in measured abundances between libraries that may reflect either biologically meaningful differences or noise introduced during sample processing. To address this problem, we independently prepared,

sequenced, and analyzed a second sample of the inoculum library (see Table S1 in the supplemental material). The comparison of these two technical replicates allowed us to directly observe the extent of artifactual variation introduced by sample processing (Fig. 3A). ORFs in the *in vivo* data set that met a strict *P* value cutoff of 0.05 and that fell entirely outside the range of variability observed between inoculum library replicates were considered candidates for significantly selected genes

Fifty-three chromosomal genes met these criteria for signifi-

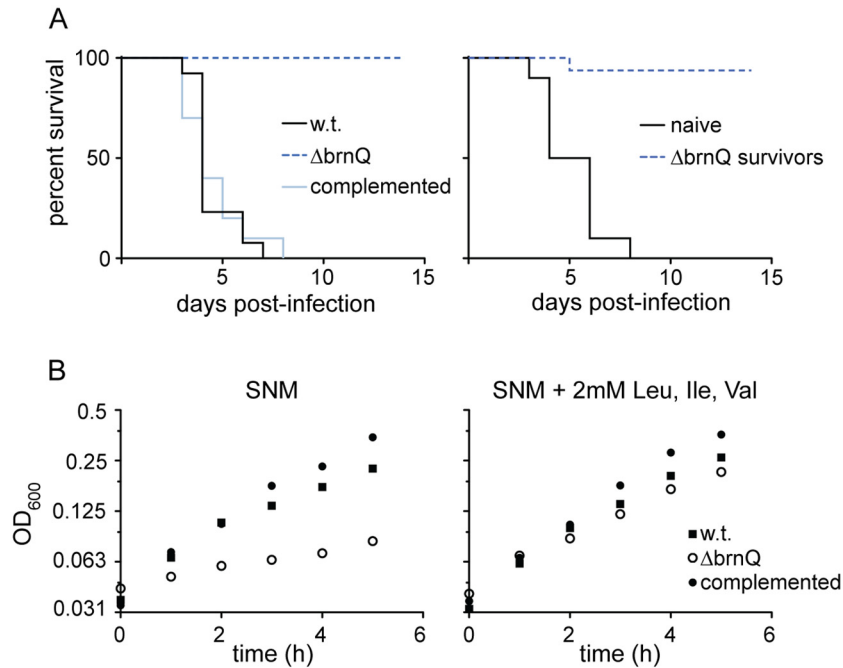


FIG 4 *Y. pestis* requires the branched-chain amino acid importer BrnQ for virulence in mice. (A) Left: subcutaneous infection with 1,000 CFU KIM1001 (w.t.) ($n = 9$), KIM1001 $\Delta brnQ$ ($\Delta brnQ$) ($n = 17$), or the complemented strain KIM1001 $\Delta brnQ$ (pSP6) (complemented) ($n = 5$). Mice infected with KIM1001 or KIM1001 $\Delta brnQ$ (pSP6) died within the first week of infection, while the mutant KIM1001 $\Delta brnQ$ strain failed to sicken or kill mice. Right: previous infection with KIM1001 $\Delta brnQ$ protected 15 out of 16 mice from subcutaneous challenge with 1,000 CFU KIM1001 28- to 30 days later. (B) Growth of the attenuated strains JG150A (w.t.), JG150A $\Delta brnQ$ ($\Delta brnQ$), and JG150A $\Delta brnQ$ (pSP6) (complemented) in the defined serum-like medium SNM alone (left) or supplemented with 2 mM leucine, isoleucine, and valine (right). Curves are representative of two independent experiments.

cant selection *in vivo* (Table 1), many of which fell into common KEGG pathways (see Table S3 in the supplemental material). These pathways include purine and pyrimidine biosynthesis, metabolism of both aromatic and certain nonaromatic amino acids, biosynthesis of secondary metabolites, and the ABC transporter category. Genes selected *in vivo* also include hypothetical genes, genes of unknown function, and annotated genes with putative functions that have not previously been implicated in *Y. pestis* infection. Notable among these are $\gamma 0661$, a hypothetical gene containing a conserved domain of unknown function, and $\gamma 1920$, encoding a homologue of the lipopolysaccharide (LPS) modification enzyme ArnD, which was recently reported to be selected in the closely related species *Yersinia pseudotuberculosis* during infection (25) (Table 1).

Branched-chain amino acid transport by BrnQ is required for *Y. pestis* virulence. The putative branched-chain amino acid importer encoded by *brnQ* ($\gamma 0981$) was among the most strongly selected genes *in vivo*, despite its apparent dispensability *in vitro* (Fig. 3A and B). A homologous importer has been reported to play a role in valine uptake during intracellular growth of *Chlamydia trachomatis* (40). To validate this observed *in vivo* fitness defect, we constructed an in-frame deletion of *brnQ* in the virulent strain KIM1001. Subcutaneous infection with 10^3 (Fig. 4A) or 10^5 (see Fig. S1 in the supplemental material) CFU of the KIM1001 $\Delta brnQ$ mutant failed to visibly sicken mice, while all mice infected with wild-type KIM1001 died within 8 days. Sixty percent of mice succumbed to infection with 10^7 CFU of this mutant (see Fig. S1), indicating a roughly 1-millionfold increase in mean lethal dose in the absence of *brnQ* (since the 50% lethal dose [LD₅₀] of wild-type

KIM1001 is <50 CFU by subcutaneous infection [41]). Complementation with the *brnQ* gene driven by its native promoter on the low-copy-number plasmid pSP6 restored virulence (Fig. 4A). Four days after subcutaneous infection with 1,000 CFU KIM1001 $\Delta brnQ$, no *Y. pestis* could be recovered from the homogenized spleens of mice ($n = 5$; limit of detection, $<10^1$ CFU/spleen).

To determine if infection with *brnQ* mutants could protect against subsequent infection, mice surviving infection with KIM1001 $\Delta brnQ$ (a dose of 10^3 CFU) were challenged 28 or 30 days after the initial infection with 10^3 CFU of wild-type KIM1001. Fifteen of the sixteen mice previously infected with KIM1001 $\Delta brnQ$ survived the challenge without visible symptoms, while all naive mice succumbed (Fig. 4A).

Notably, *brnQ* mutants were not underrepresented in the *in vitro* Tn-seq data set. To investigate this phenomenon, we reconstructed the in-frame deletion of *brnQ* in the attenuated strain JG150A, allowing us to investigate growth of the mutant under biosafety level 2 (BSL2) conditions. In accordance with the *in vitro* Tn-seq data, JG150A $\Delta brnQ$ grew as well as the wild-type control in the rich medium TB and had only a mild growth defect in PMH2, a defined medium commonly used for culturing *Y. pestis* (42) (Table 2; see also Fig. S2A and B in the supplemental material). Since *brnQ* is annotated as an ABC transporter that imports the branched-chain amino acids leucine, isoleucine, and valine, we formulated a new defined medium for culturing *Y. pestis* to probe for a deficiency in branched-chain amino acid acquisition. Serum nutritional medium (SNM) contains levels of magnesium,

TABLE 2 The *brnQ* deletion mutant grows poorly at low concentrations of branched-chain amino acids

Growth medium	Growth rate ^a		Relative fitness (<i>W</i>) ^b
	JG150A	JG150AΔ <i>brnQ</i>	
TB	0.5450 ± 0.023	0.5301 ± 0.044	0.973
SNM	0.3987 ± 0.075	0.0681 ± 0.023	0.171
SNM + 2 mM Leu, Ile, Val	0.4063 ± 0.002	0.3253 ± 0.001	0.801

^a Growth rates of the wild-type JG150A strain and the deletion mutant JG150AΔ*brnQ* were calculated from cultures at mid-log phase. Means and standard errors from a minimum of two independent experiments are shown.

^b In these experiments, relative fitness was calculated by taking the ratio of the JG150AΔ*brnQ* growth rate and the JG150A growth rate.

sodium, glucose, and all amino acids equivalent to those found in serum (see Text S1).

The growth rate of JG150AΔ*brnQ* cultured in SNM is less than one-fifth of the growth rate for wild-type JG150A in the same medium (relative fitness, 0.171). As in infection studies, complementing *brnQ* with a wild-type copy of the gene under its native promoter in *trans* restored growth of the mutant to wild-type levels (Fig. 4B). Growth could also be restored by supplementing SNM with 2 mM leucine, isoleucine, and valine—concentrations similar to those in PMH2 (Fig. 4B and Table 2). Interestingly, supplementing the medium with isoleucine and valine in the absence of leucine did not fully restore growth (see Fig. S2C in the supplemental material), despite the presence of the apparently functional alternative leucine uptake system LS in *Y. pestis* KIM (livKHMGE; y0422–y0426) (43) that has been reported to be expressed *in vivo* (7).

Glucose import by PtsG provides a competitive advantage to *Y. pestis* during infection. Recent work screening a defined panel of *Y. pestis* mutants implicated the glucose importer encoded by *ptsG* in bacterial fitness during infection (15). As with *brnQ*, the Tn-seq data set identified *ptsG* as significantly selected *in vivo*, but insertions in *ptsG* caused a much more modest reduction in relative fitness (0.693) (Table 1 and Fig. 3A and B). To assess the contribution of *ptsG* to virulence, we subcutaneously infected C57BL/6 mice with 1,000 CFU of the in-frame deletion strain KIM1001Δ*ptsG*. The course of disease with KIM1001Δ*ptsG* did not differ significantly from that with wild-type KIM1001 (Fig. 5). We therefore considered the hypothesis that the decrease in

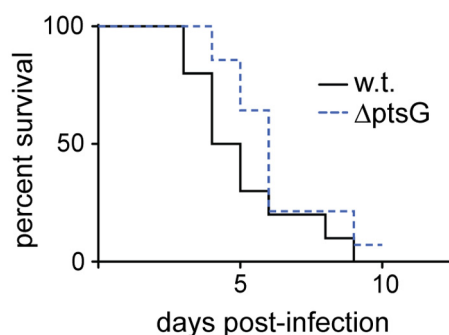


FIG 5 The glucose importer encoded by *ptsG* has little effect on *Y. pestis* virulence. Subcutaneous infections with 1,000 CFU KIM1001 (w.t.) ($n = 10$) or KIM1001Δ*ptsG* (Δ*ptsG*) ($n = 14$) were carried out. Thirteen out of fourteen mice infected with KIM1001Δ*ptsG* died, with kinetics similar to those of mice infected with KIM1001.

growth caused by inactivation of *ptsG* is insufficient to affect the outcome of infection but that *ptsG* confers a competitive fitness advantage to *Y. pestis* during growth in mammals.

We infected BALB/C and C57BL/6 mice intravenously with 10⁴ CFU of KIM1001 and KIM1001Δ*ptsG* in a 1:1 mixture. Splens were homogenized 2 and 42 h postinfection, and the proportion of *ptsG* mutants in the spleen was determined at each time point. The relative frequency of KIM1001Δ*ptsG* mutants declined significantly over the course of the experiment (Fig. 6A). On average, the proportion of KIM1001Δ*ptsG* mutants in the spleen decreased from 0.434 at 2 h postinfection (i.e., 43.4% mutants) to 0.039 (3.9%) at 42 h postinfection. Assuming constant exponential growth rates during the infection, this change in frequency corresponds to a relative fitness of 0.8 for KIM1001Δ*ptsG* relative to wild-type KIM1001, a value close to that determined from the Tn-seq experiments (Table 1).

We were able to recapitulate this phenotype *in vitro* in the defined serum-like medium SNM. Five replicate cultures were inoculated with equal numbers of the attenuated (T3SS-deficient) strains JG102 and JG102Δ*ptsG*. After 42 h of continuous log-phase growth, the proportion of *ptsG* mutants in the culture had decreased from 0.5 to an average of 0.034 (Fig. 6B). This reduction in frequency represents a relative fitness of 0.794 for the *ptsG* mutant relative to the control strain, JG102, in the same medium, very similar to the value of 0.8 observed *in vivo*. No growth defect was detected in SNM when the JG102Δ*ptsG* mutant was complemented with a low-copy-number plasmid carrying *ptsG* under control of its native promoter (see Fig. S3 and Text S1 in the supplemental material).

Because PtsG is annotated as a glucose importer, we tested whether glucose is required for the competitive advantage provided by *ptsG*. No fitness defect was detected for the *ptsG* mutant grown in the absence of glucose (Fig. 6B), consistent with the apparently neutral phenotype of *ptsG* insertion mutants in the *in vitro* Tn-seq data set (Fig. 3B). In contrast, the proportion of *ptsG* mutants in cultures containing glucose decreased on average from 0.592 to 0.266 (Fig. 6B). This decrease corresponds to a relative fitness of 0.92 for JG102Δ*ptsG* relative to wild-type JG102 in this rich culture medium, supporting the hypothesis that *ptsG* provides a competitive advantage to *Y. pestis* during infection by permitting or increasing glucose import.

Intercellular complementation *in vivo*: genes required for siderophore-mediated iron acquisition. Growth *in vivo* strongly selected against insertions in the *psn* gene (y2404), which encodes the outer membrane TonB-dependent yersiniabactin importer (44), and in *ybtA* (y2398), the regulator required for expression of *psn* and other genes in the yersiniabactin uptake system (45) (Table 1 and Fig. 3A and B). This agrees with an extensive body of literature describing the requirement for yersiniabactin-mediated iron acquisition for optimal growth under iron-limiting conditions (44, 46), including *in vivo* (4, 6, 47).

However, the genes required for biosynthesis of the yersiniabactin siderophore (Ybt) were not selected *in vitro* or *in vivo* (see Table S4 in the supplemental material). This apparent contradiction almost certainly results from intercellular complementation. Extracellular yersiniabactin has been reported to complement the growth of mutants deficient in yersiniabactin biosynthesis even in low-iron environments (44). Because our experiments were performed at a relatively high bacterial density and the vast majority of the bacterial population remains functionally wild type with

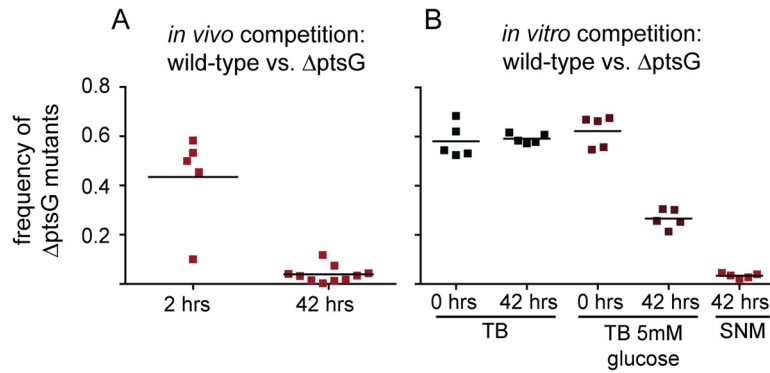


FIG 6 *ptsG* provides a competitive advantage in the presence of glucose. (A) A 10^4 -CFU dose of wild-type KIM1001 and KIM1001 $\Delta ptsG$ (mixed 1:1) was injected intravenously into BALB/C or C57BL/6 mice. The proportion of KIM1001 $\Delta ptsG$ mutants in the population of *Y. pestis* in the spleen was determined 2 and 42 h postinfection by plating on TB supplemented with 2.5 mM $CaCl_2$, 1% glucose, and 50 $\mu g/ml$ tetrazolium red. (B) The attenuated strains JG102 and JG102 $\Delta ptsG$ were mixed 1:1 in the rich medium TB, in TB supplemented with 5 mM glucose, and in the defined medium SNM ($n = 5$ for each condition). The proportion of JG102 $\Delta ptsG$ in each culture was measured before and after 42 h of log-phase growth.

respect to siderophore production, the concentration of extracellular yersiniabactin is likely high enough to provide iron to mutants deficient in Ybt synthesis.

Native *Y. pestis* plasmids. All three of the native plasmids in *Y. pestis* KIM1001 have been shown to have virulence functions in mice. To measure the contribution of plasmid genes to bacterial fitness during infection, we calculated the *in vivo* relative fitness and significance for each annotated ORF on the plasmids as described above for chromosomal genes.

pCD1 and genes of the type III secretion system. The type III secretion system encoded on the 70-kb plasmid pCD1 is essential for virulence of *Y. pestis*. We observed very strong reductions in relative fitness of mutants defective for many T3S genes (see Table S4 in the supplemental material). For example, *yscF*, which encodes the major structural subunit of the needle, was classified as strongly selected *in vivo* (relative fitness = 0; see Table S4). *lcrV*, *yopB*, and *yopD*, encoding the translocon apparatus, also had large reductions in relative fitness (0, 0.55, and 0.69). Among the secreted effectors, insertions in the genes encoding a GTPase-activating enzyme (*yopE*), a tyrosine phosphatase (*yopH*), and a regulatory effector (*yopK*) suffered clearly significant reductions in relative fitness (Fig. 7; see also Table S4). We did not detect a reduction in fitness for insertions in the effector-encoding genes *yopM* (encoding a possible inhibitor of inflammasome activation), *ypkA* (encoding a serine/threonine kinase), or *yopT* (encoding a cysteine protease). Insertions in *yopJ* (encoding an acetyltransferase) showed weak but not significant positive selection. These results are consistent with previous reports that some effectors are crucial while others appear to contribute very modestly or not at all to virulence (48–53).

pMT1. No genes on pMT1 experienced significant selection *in vivo*. pMT1 carries a gene encoding a phospholipase D, *ymt* (Y1069), that was initially thought to contribute to virulence in mice; however, the lack of apparent selection on *ymt* is in accordance with more recent reports that *ymt* primarily promotes bacterial survival in the flea vector (54) rather than enhancing virulence in mammals (55). pMT1 also carries a gene, *caf1* (Y1100), encoding the fraction 1 capsule protein, which produces abundant pili loosely associated with the cell surface. As with *ymt*, we did not detect significant selection of *caf1* *in vivo*.

pPCP1. None of the five annotated ORFs on pPCP1 experienced significant selection *in vivo*. pPCP1 encodes a single characterized virulence factor, the plasminogen activator encoded by *pla*, which plays a crucial role in progression to systemic infection following subcutaneous or intradermal infection (41, 56) but is less important in pulmonary infection (57) and has little effect following intravenous infection (58). Failure of *pla* mutants to show a fitness deficit in the Tn-seq data set is thus not surprising.

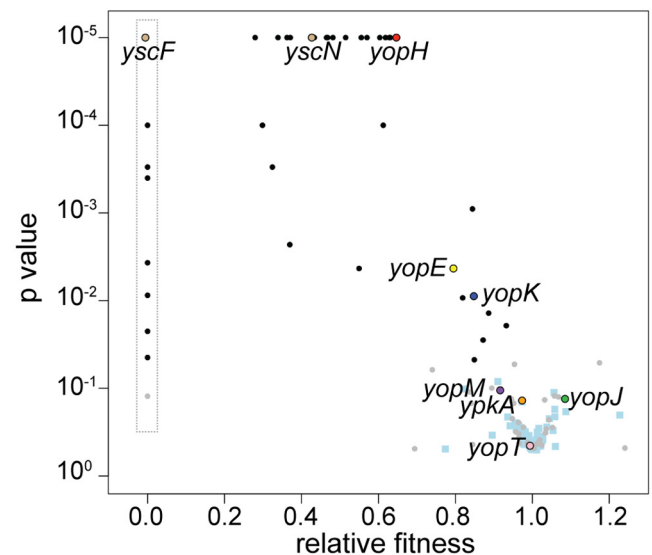


FIG 7 Many genes on the type III secretion plasmid pCD1 undergo strong selection during infection. Each gene on pCD1 was compared between two *in vitro* data sets (filled pale blue squares) or between an *in vitro* data set and the *in vivo* data set (gray circles). Genes experiencing significant selection *in vivo* are represented by black circles. Genes harboring no sequenced insertions *in vivo* in the central 90% of the ORF (relative fitness = 0) are shown in the box at the left of the plot. The effector proteins of the type III secretion system undergo variable levels of selection (red, *yopH*; yellow, *yopE*; dark blue, *yopK*; orange, *ypkA*; purple, *yopM*; pink, *yopT*; green, *yopJ*), while the ATPase (tan, *yscN*) and structural components (tan, *yscF*) undergo strong selection.

DISCUSSION

We detected a substantial fraction of the genes previously implicated in the virulence of *Y. pestis* (see Table S5 in the supplemental material). Some of the virulence genes not detected have been shown to be important via subcutaneous but not intravenous infection (e.g., *pla* and *yadBC*), while others may well have this property (*ail*, *caf1*, and *psa*; see Table S5). Alternatively, intercellular complementation may mask the requirement for *caf1* and/or *psa*, since both of these genes encode highly abundant secreted proteins. Our results are also generally in agreement with the recent study by Crimmins et al., which reports Tn-seq data for the closely related species *Y. pseudotuberculosis* following intravenous infection (25). As in our study, these investigators found crucial roles *in vivo* for purine biosynthesis (*purM*, *purH*, *purC*, and *purD*), aromatic amino acid biosynthesis (*aroA* and *aroE*), and LPS modification (*arnD*) (25). The remaining differences in our results may reflect biological differences between these two organisms, which differ in requirements for growth *in vitro* and cause very different diseases, but also reflect the increased sensitivity and resolution of our experiments, which employed a 100-fold-larger library.

A comparison of the Tn-seq data set to the *in vivo* competition data for a defined panel of *Y. pestis* mutants recently published by Pradel et al. (15) reveals several genes with reduced fitness in both experiments. Interestingly, however, there remains considerable disagreement between the candidates identified by Pradel et al. and results of the Tn-seq approach described here. In particular, Pradel et al. found that *ptsG* mutants are attenuated in a subcutaneous single-infection model, whereas we found that *ptsG* mutants remained fully virulent. It is possible that the low dose used by Pradel et al., which they report as 10 CFU, may explain this discrepancy.

Many genes experiencing significant *in vivo* selection during the Tn-seq experiment have roles in nutrient import or biosynthesis. The widespread use of rich media containing nutritional conditions not found in the host in both clinical and research settings may partly explain why these genes are often overlooked as therapeutic targets. As an illustration of this principle, the poor fitness of *brnQ* mutants *in vivo* cannot be detected on the rich medium TB but is readily apparent in media specifically designed to mimic nutritional conditions in serum. As illustrated by the strong immunity induced by infection with our *brnQ* mutant, importers required for nutrition *in vivo* may also be useful for the rational design of strains to be used as live vaccines.

Even in media recapitulating the *in vivo* environment, a growth defect *in vitro* does not always translate to reduced virulence. The behavior of *brnQ* mutants versus that of *ptsG* mutants makes clear the important distinction between fitness and virulence: the detection of reduced relative fitness by Tn-seq does not necessarily imply attenuation of the corresponding mutant. *In vivo* fitness and virulence can be distinct properties, especially when the fitness reduction is small.

With a few exceptions, Tn-seq studies reported to date present the observed effect of mutants in a given gene either as a ratio of the raw frequencies (e.g., see reference 22) or the log base 2 of this ratio (e.g., see reference 21). As we have done here, van Opijnen and Camilli (35) use the metric of relative fitness. We suggest the adoption of this measure as a standard for the presentation of Tn-seq results. The ratio of raw frequencies yields extreme values

that can be misleading. Log base 2 of these ratios is proportional to relative fitness, but the constant of proportionality will differ depending on experimental details, and hence this metric may not be directly comparable among studies. Relative fitness suffers from neither of these complications and has several additional advantages: most importantly, its readily interpreted biological meaning and its congruence with the formal definitions for the synergy or independence of mutational effects. The latter is especially useful in genetic interaction studies, in which libraries constructed in specific mutant backgrounds are to be compared with libraries constructed in the wild-type parent.

The wealth of available data on *Yersinia pestis* pathogenesis enables the critical evaluation of the Tn-seq method in the context of infection studies. For example, the intercellular complementation of the yersiniabactin siderophore system suggests that intercellular complementation may be a common phenomenon in Tn-seq and related methods. In support of this conclusion, Price et al. observed strong intercellular complementation of the *Y. pestis* T3SS in lung tissue when they applied an alternate technique for screening transposon mutant libraries (TraSH) (59). The pattern we observe in the yersiniabactin system—a cluster of genes devoted to synthesis of a secondary metabolite not under selection, coupled to a transporter under strong selection—may be a signature for intercellular complementation by a highly diffusible small molecule. In the context of pathogenesis, a lack of an observed fitness deficit in Tn-seq studies cannot be interpreted as definitive evidence that the gene in question would not be important, or even essential, if the mutant were in pure culture.

The requirement for a large inoculum to provide good coverage of the genome is perhaps the most important limitation of the Tn-seq method. One of the most important properties of *Y. pestis* is its ability to produce systemic infection following intradermal inoculation with a few bacteria; however, this problem cannot be practically addressed by Tn-seq due to bottleneck effects that reduce library diversity. As the work by Pradel et al. illustrates, a genomic-scale approach to identifying the genes required for infection via a peripheral route would be practicable only with an ordered array library orders of magnitude smaller than the random library used here and even then would require a large number of mice to limit inoculum size and overcome mouse-to-mouse variation (15). Nonetheless, as we have shown here, even very large inocula (in our case, more than 2 million LD₅₀s) can yield a wealth of data that accurately reflect the underlying biology established over many years for *Y. pestis*. The *in vivo* application of Tn-seq is clearly an approach of extraordinary power that should greatly accelerate the understanding of many pathogens. Development of adequate libraries may be a significant obstacle in many species, but effort devoted to overcoming this obstacle is very likely to be a worthwhile investment.

MATERIALS AND METHODS

Bacterial strains and growth conditions. Strains used in this study and details of strain construction are presented in Text S1 in the supplemental material. Unless otherwise specified, *E. coli* strains were cultured in Luria broth (LB) and *Y. pestis* strains in the rich medium TB, prepared to maximize plating efficiency as previously described (60). Additional experiments were performed in the defined media PMH2 (42) or SNM (see Text S1). All *Y. pestis* cultures were supplemented with 2.5 mM CaCl₂ to suppress type III secretion. Where appropriate, media were supplemented with 100 μg/ml ampicillin, 25 μg/ml zeocin, or 25 μg/ml diaminopimelic acid.

Library construction and Tn-seq. Experimental details of library generation, selection, preparation for Illumina sequencing, sequence read processing, and statistical analysis are available in Text S1 in the supplemental material. Raw sequence reads are available in the NCBI Sequence Read Archive (SRA) (<http://www.ncbi.nlm.nih.gov/Traces/sra>) under BioProject PRJNA240677, accession numbers SRX483428 (reference *in vitro* library), SRX483566 (replicate *in vitro* library), and SRX483575 (*in vivo* library).

Animal infections. This study was conducted in conformity with the Guide for the Care and Use of Laboratory Animals of the National Institutes of Health and with the review and approval of the University of Massachusetts Medical School Institutional Animal Care and Use Committee (IACUC).

C57BL/6 and BALB/C mice were infected as appropriate. All bacterial cultures used for inoculation were grown at 37°C on TB agar (TB medium with 1.5% agar) containing 2.5 mM CaCl₂ overnight prior to infection. Bacterial cells were diluted in infection-grade phosphate-buffered saline (PBS) to the desired concentration. In every case, the number of viable bacteria present in each dose was verified by dilution plating of the inoculum. Mice were monitored every 12 h for signs of illness, such as ruffled fur, shallow breathing, limping, reluctance to move, and swollen lymph nodes.

***ptsG* competition experiments.** Mice were sacrificed 2 h or 42 h following coinfection with 3 × 10³ CFU of a 1:1 mixture of KIM1001 and KIM1001Δ*ptsG*. Spleens were removed and homogenized in 0.5 ml sterile PBS. Dilutions were plated on TB agar containing 2.5 mM CaCl₂, 1% glucose, and 50 μg/ml tetrazolium red. On this medium, the wild-type strain KIM1001 forms white colonies, while colonies of KIM1001Δ*ptsG* are purple (61). *In vitro* competition experiments were performed by mixing JG102 and JG102Δ*ptsG* 1:1 and plating cultures on TB agar containing 2.5 mM CaCl₂, 1% glucose, and 50 μg/ml tetrazolium red after 0 h or 42 h of continuous log-phase growth at 37°C. The fraction of JG102Δ*ptsG* colonies was determined by calculating the fraction of purple colonies on these dilution plates.

Because the JG102 strain and the complemented strain JG102Δ*ptsG*(pZS*13luc:*ptsG*) both ferment glucose, both form white colonies on TB agar supplemented with 1% glucose and 50 μg/ml tetrazolium red. *In vitro* competition experiments with the complemented strain were therefore performed against the control strain, JG102Δ*xytB*(pZS*13luc), cultured in the presence of 100 μg/ml ampicillin. Dilutions were plated on TB agar supplemented with 2.5 mM CaCl₂, 1% xylose, and 30 μg/ml neutral red after 0 h or 42 h of continuous log-phase growth at 37°C. On these plates, the complemented strain, JG102Δ*ptsG*(pZS*13luc:*ptsG*), forms white colonies, and the control strain, JG102Δ*xytB*(pZS*13luc), forms red colonies. The fraction of JG102Δ*ptsG*(pZS*13luc:*ptsG*) colonies was determined by calculating the fraction of red colonies on these dilution plates.

The change in the growth rate was determined by plotting the natural log of the ratio of the *ptsG* mutant to the wild-type strain over time and calculating the slope by linear regression. Absolute change in growth rate was applied to the measured growth rate for the wild-type strain to determine mutant growth rates.

SUPPLEMENTAL MATERIAL

Supplemental material for this article may be found at <http://mbio.asm.org/lookup/suppl/doi:10.1128/mBio.01385-14/-/DCSupplemental>.

- Text S1, PDF file, 0.4 MB.
- Text S2, PDF file, 0.2 MB.
- Table S1, XLSX file, 0.5 MB.
- Table S2, XLSX file, 0.7 MB.
- Table S3, XLSX file, 0.1 MB.
- Table S4, PDF file, 0.1 MB.
- Table S5, PDF file, 0.1 MB.
- Figure S1, TIF file, 2.1 MB.
- Figure S2, TIF file, 5.2 MB.
- Figure S3, TIF file, 1.3 MB.

ACKNOWLEDGMENTS

This work was supported by the NIH/NIAID grant 5U01AI078073 to S.L. and by unrestricted research funds from the University of Massachusetts Medical School to J.D.G.

We thank Christopher Sasseti, Jeff Gawronski, and Brian Akerley for sharing their tremendously helpful Tn-seq expertise and Alice Li and Jarukit Ed Long for their technical advice. We also thank Thomas Ioerger for the hidden Markov model, Ellen Kittler for Illumina sequencing support, Dieter Schifferli and Kenan Murphy for generously providing genetic tools, and Christina Baer for critical reading of the manuscript.

REFERENCES

- Higuchi K, Kupferberg LL, Smith JL. 1959. Studies on the nutrition and physiology of *Pasteurella pestis*. III. Effects of calcium ions on the growth of virulent and avirulent strains of *Pasteurella pestis*. *J. Bacteriol.* 77: 317–321.
- Rosqvist R, Magnusson KE, Wolf-Watz H. 1994. Target cell contact triggers expression and polarized transfer of *Yersinia YopE* cytotoxin into mammalian cells. *EMBO J.* 13:964–972.
- Haag H, Hantke K, Drechsel H, Stojiljkovic I, Jung G, Zähler H. 1993. Purification of yersiniabactin: a siderophore and possible virulence factor of *Yersinia enterocolitica*. *J. Gen. Microbiol.* 139:2159–2165. <http://dx.doi.org/10.1099/00221287-139-9-2159>.
- Bearden SW, Fetherston JD, Perry RD. 1997. Genetic organization of the yersiniabactin biosynthetic region and construction of avirulent mutants in *Yersinia pestis*. *Infect. Immun.* 65:1659–1668.
- Burrows TW, Jackson S. 1956. The pigmentation of *Pasteurella pestis* on a defined medium containing haemin. *Br. J. Exp. Pathol.* 37:570–576.
- Burrows TW, Jackson S. 1956. The virulence-enhancing effect of iron on nonpigmented mutants of virulent strains of *Pasteurella pestis*. *Br. J. Exp. Pathol.* 37:577–583.
- Lathem WW, Crosby SD, Miller VL, Goldman WE. 2005. Progression of primary pneumonic plague: a mouse model of infection, pathology, and bacterial transcriptional activity. *Proc. Natl. Acad. Sci. U. S. A.* 102: 17786–17791. <http://dx.doi.org/10.1073/pnas.0506840102>.
- Sebbane F, Lemaitre N, Sturdevant DE, Rebeil R, Virtaneva K, Porcella SF, Hinnebusch BJ. 2006. Adaptive response of *Yersinia pestis* to extracellular factors of innate immunity during bubonic plague. *Proc. Natl. Acad. Sci. U. S. A.* 103:11766–11771. <http://dx.doi.org/10.1073/pnas.0601182103>.
- Han Y, Qiu J, Guo Z, Gao H, Song Y, Zhou D, Yang R. 2007. Comparative transcriptomics in *Yersinia pestis*: a global view of environmental modulation of gene expression. *BMC Microbiol.* 7:96. <http://dx.doi.org/10.1186/1471-2180-7-96>.
- Chauvaux S, Rosso ML, Frangeul L, Lacroix C, Labarre L, Schiavo A, Marceau M, Dillies MA, Foulon J, Coppée JY, Médigue C, Simonet M, Carniel E. 2007. Transcriptome analysis of *Yersinia pestis* in human plasma: an approach for discovering bacterial genes involved in septicemic plague. *Microbiology* 153:3112–3124. <http://dx.doi.org/10.1099/mic.0.2007/006213-0>.
- Vadyvaloo V, Jarrett C, Sturdevant DE, Sebbane F, Hinnebusch BJ. 2010. Transit through the flea vector induces a pretransmission innate immunity resistance phenotype in *Yersinia pestis*. *PLoS Pathog.* 6:e1000783. <http://dx.doi.org/10.1371/journal.ppat.1000783>.
- Sasseti CM, Boyd DH, Rubin EJ. 2001. Comprehensive identification of conditionally essential genes in mycobacteria. *Proc. Natl. Acad. Sci. U. S. A.* 98:12712–12717. <http://dx.doi.org/10.1073/pnas.231275498>.
- Rengarajan J, Bloom BR, Rubin EJ. 2005. Genome-wide requirements for *Mycobacterium tuberculosis* adaptation and survival in macrophages. *Proc. Natl. Acad. Sci. U. S. A.* 102:8327–8332. <http://dx.doi.org/10.1073/pnas.0503272102>.
- de Vries SP, Eleveld MJ, Hermans PW, Bootsma HJ. 2013. Characterization of the molecular interplay between *Moraxella catarrhalis* and human respiratory tract epithelial cells. *PLoS One* 8:e72193. <http://dx.doi.org/10.1371/journal.pone.0072193>.
- Pradel E, Lemaitre N, Merchez M, Ricard I, Rebol A, Dewitte A, Sebbane F. 2014. New insights into how *Yersinia pestis* adapts to its mammalian host during bubonic plague. *PLoS Pathog.* 10:e1004029. <http://dx.doi.org/10.1371/journal.ppat.1004029>.
- Gawronski JD, Wong SM, Giannoukos G, Ward DV, Akerley BJ. 2009. Tracking insertion mutants within libraries by deep sequencing and a

- genome-wide screen for Haemophilus genes required in the lung. Proc. Natl. Acad. Sci. U. S. A. 106:16422–16427. <http://dx.doi.org/10.1073/pnas.0906627106>.
17. Langridge GC, Phan MD, Turner DJ, Perkins TT, Parts L, Haase J, Charles I MDJ, Peters SE, Dougan G, Wain J, Parkhill J, Turner AK. 2009. Simultaneous assay of every Salmonella Typhi gene using one million transposon mutants. Genome Res. 19:2308–2316. <http://dx.doi.org/10.1101/gr.097097.109>.
 18. Goodman AL, McNulty NP, Zhao Y, Leip D, Mitra RD, Lozupone CA, Knight R, Gordon JI. 2009. Identifying genetic determinants needed to establish a human gut symbiont in its habitat. Cell Host Microbe 6:279–289. <http://dx.doi.org/10.1016/j.chom.2009.08.003>.
 19. van Opijnen T, Bodi KL, Camilli A. 2009. Tn-seq: high-throughput parallel sequencing for fitness and genetic interaction studies in microorganisms. Nat. Methods 6:767–772. <http://dx.doi.org/10.1038/nmeth.1377>.
 20. Zhang YJ, Ioerger TR, Huttenhower C, Long JE, Sasseti CM, Sacchetti JC, Rubin EJ. 2012. Global assessment of genomic regions required for growth in Mycobacterium tuberculosis. PLoS Pathog. 8:e1002946. <http://dx.doi.org/10.1371/journal.ppat.1002946>.
 21. Griffin JE, Gawronski JD, DeJesus MA, Ioerger TR, Akerley BJ, Sasseti CM. 2011. High-resolution phenotypic profiling defines genes essential for mycobacterial growth and cholesterol catabolism. PLoS Pathog. 7:e1002251. <http://dx.doi.org/10.1371/journal.ppat.1002251>.
 22. Gallagher LA, Shendure J, Manoil C. 2011. Genome-scale identification of resistance functions in *Pseudomonas aeruginosa* using Tn-seq. mBio 2(1):e00315-00310. <http://dx.doi.org/10.1128/mBio.00315-10>.
 23. Mann B, van Opijnen T, Wang J, Obert C, Wang YD, Carter R, McGoldrick DJ, Ridout G, Camilli A, Tuomanen EI, Rosch JW. 2012. Control of virulence by small RNAs in *Streptococcus pneumoniae*. PLoS Pathog. 8:e1002788. <http://dx.doi.org/10.1371/journal.ppat.1002788>.
 24. Khatiwara A, Jiang T, Sung SS, Dawoud T, Kim JN, Bhattacharya D, Kim HB, Ricke SC, Kwon YM. 2012. Genome scanning for conditionally essential genes in *Salmonella enterica* serotype Typhimurium. Appl. Environ. Microbiol. 78:3098–3107. <http://dx.doi.org/10.1128/AEM.06865-11>.
 25. Crimmins GT, Mohammadi S, Green ER, Bergman MA, Isberg RR, Mecsas J. 2012. Identification of MrtAB, an ABC transporter specifically required for *Yersinia pseudotuberculosis* to colonize the mesenteric lymph nodes. PLoS Pathog. 8:e1002828. <http://dx.doi.org/10.1371/journal.ppat.1002828>.
 26. van Opijnen T, Camilli A. 2012. A fine scale phenotype-genotype virulence map of a bacterial pathogen. Genome Res. 22:2541–2551. <http://dx.doi.org/10.1101/gr.137430.112>.
 27. Dong TG, Ho BT, Yoder-Himes DR, Mekalanos JJ. 2013. Identification of T6SS-dependent effector and immunity proteins by Tn-seq in *Vibrio cholerae*. Proc. Natl. Acad. Sci. U. S. A. 110:2623–2628. <http://dx.doi.org/10.1073/pnas.1222783110>.
 28. Baugh L, Gallagher LA, Patrapuvich R, Clifton MC, Gardberg AS, Edwards TE, Armour B, Begley DW, Dieterich SH, Dranow DM, Abendroth J, Fairman JW, Fox D, III, Staker BL, Phan I, Gillespie A, Choi R, Nakazawa-Hewitt S, Nguyen MT, Napuli A, Barrett L, Buchko GW, Stacy R, Myler PJ, Stewart LJ, Manoil C, Van Voorhis WC. 2013. Combining functional and structural genomics to sample the essential Burkholderia struome. PLoS One 8:e53851. <http://dx.doi.org/10.1371/journal.pone.0053851>.
 29. Chao MC, Pritchard JR, Zhang YJ, Rubin EJ, Livny J, Davis BM, Waldor MK. 2013. High-resolution definition of the *Vibrio cholerae* essential gene set with hidden Markov model-based analyses of transposon-insertion sequencing data. Nucleic Acids Res. 41:9033–9048. <http://dx.doi.org/10.1093/nar/gkt654>.
 30. Subashchandrabose S, Smith SN, Spurbeck RR, Kole MM, Mobley HLT. 2013. Genome-wide detection of fitness genes in uropathogenic *Escherichia coli* during systemic infection. PLoS Pathog. 9:e1003788. <http://dx.doi.org/10.1371/journal.ppat.1003788>.
 31. Zhang YJ, Reddy MC, Ioerger TR, Rothchild AC, Dartois V, Schuster BM, Trauner A, Wallis D, Galaviz S, Huttenhower C, Sacchetti JC, Behar SM, Rubin EJ. 2013. Tryptophan biosynthesis protects mycobacteria from CD4 T-cell-mediated killing. Cell 155:1296–1308. <http://dx.doi.org/10.1016/j.cell.2013.10.045>.
 32. Lampe DJ, Churchill ME, Robertson HM. 1996. A purified mariner transposase is sufficient to mediate transposition in vitro. EMBO J. 15:5470–5479.
 33. Rubin EJ, Akerley BJ, Novik VN, Lampe DJ, Husson RN, Mekalanos JJ. 1999. In vivo transposition of mariner-based elements in enteric bacteria and mycobacteria. Proc. Natl. Acad. Sci. U. S. A. 96:1645–1650. <http://dx.doi.org/10.1073/pnas.96.4.1645>.
 34. Zomer A, Burghout P, Bootsma HJ, Hermans PW, van Hijum SA. 2012. ESSENTIALS: software for rapid analysis of high throughput transposon insertion sequencing data. PLoS One 7:e43012. <http://dx.doi.org/10.1371/journal.pone.0043012>.
 35. van Opijnen T, Camilli A. 2013. Transposon insertion sequencing: a new tool for systems-level analysis of microorganisms. Nat. Rev. Microbiol. 11:435–442. <http://dx.doi.org/10.1038/nrmicro3033>.
 36. DeJesus MA, Ioerger TR. 2013. A hidden Markov model for identifying essential and growth-defect regions in bacterial genomes from transposon insertion sequencing data. BMC Bioinformatics 14:303. <http://dx.doi.org/10.1186/1471-2105-14-303>.
 37. Kanehisa M, Goto S. 2000. KEGG: Kyoto encyclopedia of genes and genomes. Nucleic Acids Res. 28:27–30. <http://dx.doi.org/10.1093/nar/28.7.e27>.
 38. Aird D, Ross MG, Chen WS, Danielsson M, Fennell T, Russ C, Jaffe DB, Nusbaum C, Gnirke A. 2011. Analyzing and minimizing PCR amplification bias in Illumina sequencing libraries. Genome Biol. 12:R18. <http://dx.doi.org/10.1186/gb-2011-12-s1-p18>.
 39. Michiels T, Wattiau P, Brasseur R, Ruyschaert JM, Cornelis G. 1990. Secretion of Yop proteins by yersiniae. Infect. Immun. 58:2840–2849.
 40. Braun PR, Al-Younes H, Gussmann J, Klein J, Schneider E, Meyer TF. 2008. Competitive inhibition of amino acid uptake suppresses chlamydial growth: involvement of the chlamydial amino acid transporter BrnQ. J. Bacteriol. 190:1822–1830. <http://dx.doi.org/10.1128/JB.01240-07>.
 41. Sodeinde OA, Subrahmanyam YV, Stark K, Quan T, Bao Y, Goguen JD. 1992. A surface protease and the invasive character of plague. Science 258:1004–1007. <http://dx.doi.org/10.1126/science.1439793>.
 42. Gong S, Bearden SW, Geoffroy VA, Fetherston JD, Perry RD. 2001. Characterization of the *Yersinia pestis* Yfu ABC inorganic iron transport system. Infect. Immun. 69:2829–2837. <http://dx.doi.org/10.1128/IAI.67.5.2829-2837.2001>.
 43. Adams MD, Wagner LM, Graddis TJ, Landick R, Antonucci TK, Gibson AL, Oxender DL. 1990. Nucleotide sequence and genetic characterization reveal six essential genes for the LIV-I and LS transport systems of *Escherichia coli*. J. Biol. Chem. 265:11436–11443.
 44. Fetherston JD, Lillard JW, Jr, Perry RD. 1995. Analysis of the pesticin receptor from *Yersinia pestis*: role in iron-deficient growth and possible regulation by its siderophore. J. Bacteriol. 177:1824–1833.
 45. Fetherston JD, Bearden SW, Perry RD. 1996. YbtA, an AraC-type regulator of the *Yersinia pestis* pesticin/yersiniabactin receptor. Mol. Microbiol. 22:315–325. <http://dx.doi.org/10.1046/j.1365-2958.1996.00118.x>.
 46. Sikkema DJ, Brubaker RR. 1987. Resistance to pesticin, storage of iron, and invasion of HeLa cells by yersiniae. Infect. Immun. 55:572–578.
 47. Fetherston JD, Kirillina O, Bobrov AG, Paultley JT, Perry RD. 2010. The yersiniabactin transport system is critical for the pathogenesis of bubonic and pneumonic plague. Infect. Immun. 78:2045–2052. <http://dx.doi.org/10.1128/IAI.01236-09>.
 48. Straley SC, Cibull ML. 1989. Differential clearance and host-pathogen interactions of YopE⁻ and YopK⁻ YopL⁻ *Yersinia pestis* in BALB/c mice. Infect. Immun. 57:1200–1210.
 49. Kerschen EJ, Cohen DA, Kaplan AM, Straley SC. 2004. The plague virulence protein YopM targets the innate immune response by causing a global depletion of NK cells. Infect. Immun. 72:4589–4602. <http://dx.doi.org/10.1128/IAI.72.8.4589-4602.2004>.
 50. Peters KN, Dhariwala MO, Hughes Hanks JM, Brown CR, Anderson DM. 2013. Early apoptosis of macrophages modulated by injection of *Yersinia pestis* YopK promotes progression of primary pneumonic plague. PLoS Pathog. 9:e1003324. <http://dx.doi.org/10.1371/journal.ppat.1003324>.
 51. McPhee JB, Mena P, Bliska JB. 2010. Delineation of regions of the *Yersinia* YopM protein required for interaction with the RSK1 and PRK2 host kinases and their requirement for interleukin-10 production and virulence. Infect. Immun. 78:3529–3539. <http://dx.doi.org/10.1128/IAI.00269-10>.
 52. Zauberman A, Cohen S, Mamroud E, Flashner Y, Tidhar A, Ber R, Elhanany E, Shafferman A, Velan B. 2006. Interaction of *Yersinia pestis* with macrophages: limitations in YopJ-dependent apoptosis. Infect. Immun. 74:3239–3250. <http://dx.doi.org/10.1128/IAI.00097-06>.
 53. Brodsky IE, Medzhitov R. 2008. Reduced secretion of YopJ by *Yersinia*

- limits *in vivo* cell death but enhances bacterial virulence. *PLoS Pathog.* 4:e1000067. <http://dx.doi.org/10.1371/journal.ppat.1000067>.
54. Hinnebusch BJ, Rudolph AE, Cherepanov P, Dixon JE, Schwan TG, Forsberg A. 2002. Role of *Yersinia* murine toxin in survival of *Yersinia pestis* in the midgut of the flea vector. *Science* 296:733–735. <http://dx.doi.org/10.1126/science.1069972>.
 55. Hinnebusch J, Cherepanov P, Du Y, Rudolph A, Dixon JD, Schwan T, Forsberg A. 2000. Murine toxin of *Yersinia pestis* shows phospholipase D activity but is not required for virulence in mice. *Int. J. Med. Microbiol.* 290:483–487. [http://dx.doi.org/10.1016/S1438-4221\(00\)80070-3](http://dx.doi.org/10.1016/S1438-4221(00)80070-3).
 56. Sebbane F, Jarrett CO, Gardner D, Long D, Hinnebusch BJ. 2006. Role of the *Yersinia pestis* plasminogen activator in the incidence of distinct septicemic and bubonic forms of flea-borne plague. *Proc. Natl. Acad. Sci. U. S. A.* 103:5526–5530. <http://dx.doi.org/10.1073/pnas.0509544103>.
 57. Lathem WW, Price PA, Miller VL, Goldman WE. 2007. A plasminogen-activating protease specifically controls the development of primary pneumonic plague. *Science* 315:509–513. <http://dx.doi.org/10.1126/science.1137195>.
 58. Brubaker RR, Beesley ED, Surgalla MJ. 1965. *Pasteurella pestis*: role of pesticin I and iron in experimental plague. *Science* 149:422–424. <http://dx.doi.org/10.1126/science.149.3682.422>.
 59. Price PA, Jin J, Goldman WE. 2012. Pulmonary infection by *Yersinia pestis* rapidly establishes a permissive environment for microbial proliferation. *Proc. Natl. Acad. Sci. U. S. A.* 109:3083–3088. <http://dx.doi.org/10.1073/pnas.1112729109>.
 60. Pouliot K, Pan N, Wang S, Lu S, Lien E, Goguen JD. 2007. Evaluation of the role of LcrV-Toll-like receptor 2-mediated immunomodulation in the virulence of *Yersinia pestis*. *Infect. Immun.* 75:3571–3580. <http://dx.doi.org/10.1128/IAI.01644-06>.
 61. Miller JH. 1972. Behavior of mutants on indicator plates, p 47–55. *In* Experiments in molecular genetics. Cold Spring Harbor Laboratory, New York, NY.
 62. Stothard P, Wishart DS. 2005. Circular genome visualization and exploration using CGView. *Bioinformatics* 21:537–539. <http://dx.doi.org/10.1093/bioinformatics/bti054>.
 63. Robinson JT, Thorvaldsdóttir H, Winckler W, Guttman M, Lander ES, Getz G, Mesirov JP. 2011. Integrative genomics viewer. *Nat. Biotechnol.* 29:24–26. <http://dx.doi.org/10.1038/nbt.1754>.
 64. Thorvaldsdóttir H, Robinson JT, Mesirov JP. 2013. Integrative Genomics Viewer (IGV): high-performance genomics data visualization and exploration. *Brief. Bioinform.* 14:178–192. <http://dx.doi.org/10.1093/bib/bbs017>.
 65. Apirion D, Lassar AB. 1978. A conditional lethal mutant of *Escherichia coli* which affects the processing of ribosomal RNA. *J. Biol. Chem.* 253:1738–1742.
 66. McDowall KJ, Cohen SN. 1996. The N-terminal domain of the rne gene product has RNase E activity and is non-overlapping with the arginine-rich RNA-binding site. *J. Mol. Biol.* 255:349–355. <http://dx.doi.org/10.1006/jmbi.1996.0027>.
 67. Kaberdin VR, Miczak A, Jakobsen JS, Lin-Chao S, McDowall KJ, von Gabain A. 1998. The endoribonucleolytic N-terminal half of *Escherichia coli* RNase E is evolutionarily conserved in *Synechocystis* sp. and other bacteria but not the C-terminal half, which is sufficient for degradosome assembly. *Proc. Natl. Acad. Sci. U. S. A.* 95:11637–11642. <http://dx.doi.org/10.1073/pnas.95.20.11637>.
 68. Majdalani N, Gottesman S. 2005. The Rcs phosphorelay: a complex signal transduction system. *Annu. Rev. Microbiol.* 59:379–405. <http://dx.doi.org/10.1146/annurev.micro.59.050405.101230>.